

# Modeling of Titania Nanoparticle Accumulation at the Open End of Single-Walled Carbon Nanotubes Prior to TiO<sub>2</sub> Encapsulation

Duangkamon Baowan<sup>1,\*</sup>, Darapond Triampo<sup>2</sup>, and Wannapong Triampo<sup>3</sup>

<sup>1</sup>Department of Mathematics, Faculty of Science, Mahidol University, Bangkok 10400 Thailand;  
Centre of Excellence in Mathematics, CHE, 328 Si Ayutthaya Road, Bangkok 10400 Thailand

<sup>2</sup>Department of Chemistry, Center of Excellence for Innovation in Chemistry, Faculty of Science,  
Mahidol University, Bangkok 10400 Thailand

<sup>3</sup>Biophysics Group, Center of Excellence for Vectors and Vector-Borne Diseases, Department of Physics, Faculty of Science,  
Mahidol University, Bangkok 10400 Thailand; ThEP Center, CHE, 328 Si Ayutthaya Road, Bangkok 10400 Thailand

Carbon nanotubes (CNTs) and titanium dioxide (TiO<sub>2</sub>) are perhaps the most well-known nanoparticles. The encapsulation of TiO<sub>2</sub> into CNT could provide ideas for the development of targeted drug delivery systems. It is intuitively understood that due to particle size limitation, the relatively large size of TiO<sub>2</sub> prevents its encapsulation into CNT. However, it could be possible for TiO<sub>2</sub> to encapsulate when those two types of particles are still of comparable size. Motivated by experimental results, the aim of this paper is to utilize the Lennard-Jones (6–12) potential function and applied mathematical modeling tools to understand why TiO<sub>2</sub> nanoparticles aggregate at only one side of the carbon nanotube in order to be encapsulated into the tube (which is part of the main problem surrounding the encapsulation of TiO<sub>2</sub> nanoparticles into SWNT). The theoretical prediction suggests that TiO<sub>2</sub> particles are likely to cluster together since the energy level between two TiO<sub>2</sub> molecules and a carbon nanotube is lower than that between a TiO<sub>2</sub> molecule and a carbon nanotube. This work could be considered as one of the first step models to be used with the analytic approach before developing more complicate ones.

**Keywords:** Carbon Nanotubes, Titanium Dioxide, Lennard-Jones Potential.

## 1. INTRODUCTION

Carbon nanotubes (CNTs) and titanium dioxide (TiO<sub>2</sub>) are perhaps the most well-known nanoparticles studied to date. Single-walled carbon nanotubes (SWNTs) are of great interest because of their unusual and unique physical, chemical, and electronic properties, which make them a promising material for developing nanodevices.<sup>1,2</sup> Researchers expect that SWNTs can provide unique opportunities for the nanoscale engineering of novel one-dimensional systems, created by the self-assembly of the molecules inside the SWNT's hollow core. Materials confined in such small cavities are expected to show novel features that are not observed in bulk materials.<sup>3–5</sup> Among this class of materials, SWNTs filled with fullerenes (e.g., C<sub>60</sub>), known as “peapods,” have attracted considerable attention. The composite nature of peapod materials raises the exciting possibility of a nanoscale material that can be tailored

to a particular electronic and mechanical function. However, there is still no clear understanding of the formation mechanisms of nanopeapods.

Researching the unique properties that underlie a distinguishable system versus a micro-scale or bulk system involves examining van der Waals interaction force and the large surface to volume ratio of the nanoparticles. For the latter, titanium dioxide or titania (TiO<sub>2</sub>) has attracted great attention as an alternative material for water and air purification, and photocatalytic sterilization in the food and environmental industries.<sup>6,7</sup> It has been intensively used on a wide spectrum of organisms, including bacteria,<sup>8</sup> fungi, algae, virus,<sup>9,10</sup> and cancer cells.<sup>11,12</sup> When TiO<sub>2</sub> absorbs ultraviolet A or UV-A light with a wavelength less than 385 nm, or an energy greater than the band gap of the TiO<sub>2</sub>, it generates electron–hole pairs and migrates to the surface through diffusion and drift,<sup>13</sup> while in competition with a multitude of trapping and recombination events in the lattice bulk. On the photocatalyst surface, TiO<sub>2</sub> particles yield superoxide radicals (O<sub>2</sub><sup>•-</sup>)

\* Author to whom correspondence should be addressed.

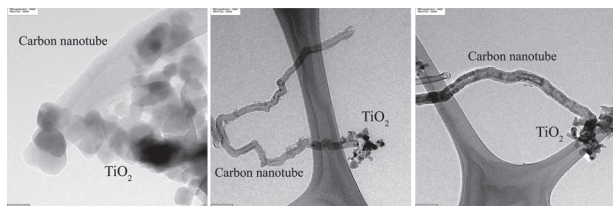


**Fig. 1.** TEM micrographs of typical TiO<sub>2</sub> nanoparticle aggregation on one end of the carbon nanotube.

and hydroxyl radicals ( $\bullet\text{OH}$ ) that can initiate oxidants.<sup>14</sup> The hydroxyl radicals are highly active particularly during the oxidation of organic substances and the inactivation of bacteria and viruses.<sup>15</sup> Most studies conclude that  $\bullet\text{OH}$  is the main cause of the bactericidal effect of photocatalysis,<sup>16,17</sup> but the mechanical basis for this effect is not well established—even though the surface properties of TiO<sub>2</sub> are well-known because this solid has been widely investigated using a variety of physicochemical methods.

Having realized what could be a high impact research study, namely investigating carbon nanotube-based hybrid materials in combination with TiO<sub>2</sub>, we considered the feasibility and optimality of encapsulating TiO<sub>2</sub> nanoparticles into SWNT. We wanted to explore whether a cluster of TiO<sub>2</sub> is an energetically favorable form for the particles to enter into the carbon nanotubes, since experimental results (see Fig. 1) showed that when the radius of the TiO<sub>2</sub> nanoparticles are smaller than that of the SWNT, the TiO<sub>2</sub> molecules aggregate at only one side of the carbon nanotube in order to be encapsulated into the tube. In this paper, we employ the Lennard-Jones potential function via applied mathematical techniques to determine the interaction energy of the TiO<sub>2</sub>–carbon nanotube system, with the aim of explaining the findings of our experiment. This could be considered as one of the first step models to be used with the analytic approach before developing more complicate ones.

## 2. EXPERIMENTAL AND THEORETICAL PREDICTIONS

We performed well-mixing experiments using TiO<sub>2</sub> and carbon nanotubes. TiO<sub>2</sub> nanoparticles (Degussa-P25) were obtained from Degussa (Thailand) Co., Ltd. Carbon nanotubes were given to us from Singjai's group.<sup>18</sup> Carbon nanotubes were ground for approximately 1 hour using a ball mill. This was done to reduce the length of the tubes. Indeed the chemical, physical, and biological properties of nanotubes are closely related to nanotube geometry. Reducing the distribution of nanotube dimensions remains a major technical challenge in carbon nanotube processing. To physically see what happened to the mixing system, we performed transmission electron microscopy (TEM) sample preparation and analysis. TEM micrographs were taken using a JEOL, JEM-2010 operating at 200 kV. Samples

were prepared by briskly shaking dry TiO<sub>2</sub> nanoparticles with dry MWNT (ratio of 1:1) in a 10 mL vial. After shaking the vial for 10 times, a TEM holey carbon-coated grid was dipped into the mixture and tapped to eliminate excess powder that was not attached strongly to the grid. At least 5 TEM samples were made, and at least 10 micrographs of each of the TEM samples were investigated for the analysis. The micrographs shown were representative of the analysis.

As seen in Figure 1, TEM micrographs show typical TiO<sub>2</sub> nanoparticle aggregation at one end of the carbon nanotube, which is quite stable. These experimental results are very reproducible. In addition, it is consistent with our analytic results, which predicts that the energetically favorable configuration happens to be a one-end aggregation of TiO<sub>2</sub>. From an interaction view point, this may be due to the fact that it requires less energy for TiO<sub>2</sub> to overcome the potential barrier of the like-particle interaction (TiO<sub>2</sub>–TiO<sub>2</sub>) in comparison with unlike-particle interaction (TiO<sub>2</sub>–CNT), which is dominated by the van der Waals force. It is noted that due to particle size limitation, the relatively large size of TiO<sub>2</sub> prevents its encapsulation into CNT. However, it is not trivial for us to consider that it could happen when those two types of particles are still comparable. More experimental evidence, such as atomic force characterization (AFM), may be found useful.

To better understand our experimental result, we utilize the Lennard-Jones potential function<sup>19</sup> to determine the interaction energy between a TiO<sub>2</sub> molecule and a carbon nanotube. On assuming that the interatomic interactions can be modeled by smearing the atoms uniformly across surfaces, the continuum approach is employed, which can be given as:

$$U = \eta_1 \eta_2 \iint \left( -\frac{A}{\rho^6} + \frac{B}{\rho^{12}} \right) dS_1 dS_2 \quad (1)$$

where  $\eta_1$  and  $\eta_2$  are the mean atomic surface densities of atoms on each molecule,  $\rho$  denotes the distance between two typical surface elements  $dS_1$  and  $dS_2$  on each molecule, and  $A$  and  $B$  are attractive and repulsive Lennard-Jones constants, respectively.

As observed in the experiment, TiO<sub>2</sub> can be modeled as a spherical particle, and carbon nanotube is assumed to be a cylindrical tube. Consequently, we want to determine the interaction energy between a sphere and a perfect cylinder, and between two spheres and a perfect cylinder, as illustrated in Figure 2, where they are assumed to be co-axially located. With reference to a rectangular Cartesian coordinate system ( $x, y, z$ ) with its origin located at the tube end, a typical point on the surface of the tube has the coordinate ( $b \cos, b \sin, z$ ), where  $b$  is the tube radius and is assumed to be semi-finite in length. Similarly, with reference to the same rectangular Cartesian coordinate system ( $x, y, z$ ), the center of the spherical TiO<sub>2</sub> has coordinates ( $0, 0, Z$ ) where  $Z$  is the distance in the axial direction,

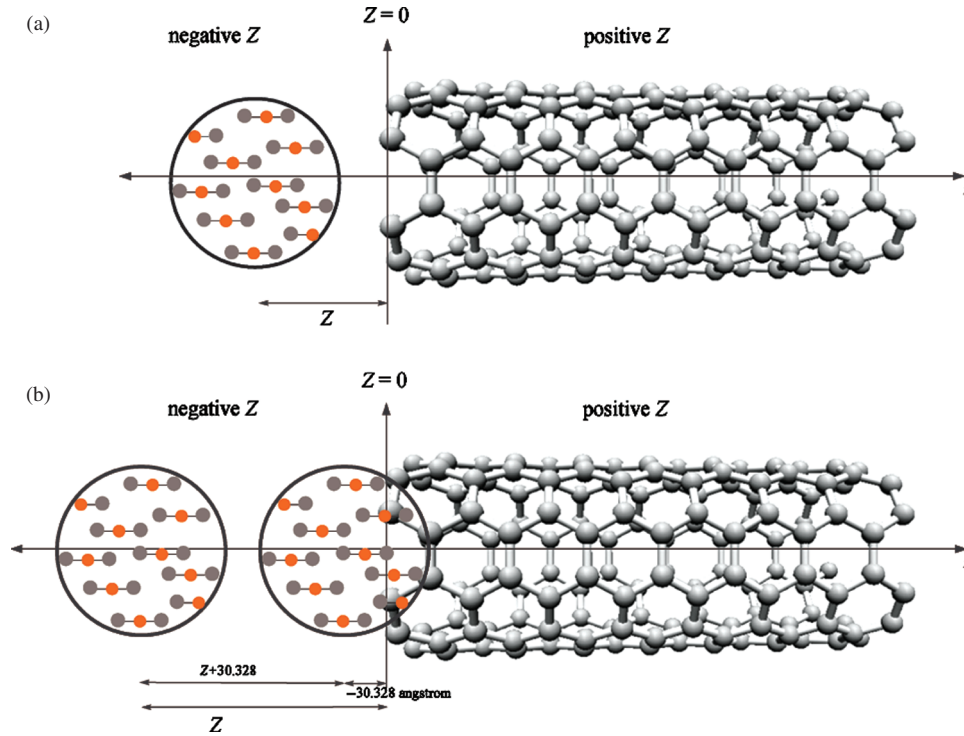


Fig. 2. Model formations for (a) TiO<sub>2</sub>-tube and (b) TiO<sub>2</sub>-TiO<sub>2</sub>-tube interactions.

which can be either positive (inside the tube) or negative (outside the tube). Thus the distance between the center of the TiO<sub>2</sub> and a typical point on the tube is given as:

$$\rho^2 = b^2 + (z - Z)^2$$

Utilizing the Lennard-Jones potential function and the continuum approximation, the total potential energy can be written as:

$$\begin{aligned} U &= E_{\text{tube-ball}}(\rho) \\ &= \pi ab \eta_1 \eta_2 \int_{-\pi}^{\pi} \int_0^{\infty} \frac{1}{\rho} \left[ \frac{A}{2} \left( \frac{1}{(\rho+a)^4} - \frac{1}{(\rho-a)^4} \right) \right. \\ &\quad \left. - \frac{B}{5} \left( \frac{1}{(\rho+a)^{10}} - \frac{1}{(\rho-a)^{10}} \right) \right] \quad (2) \end{aligned}$$

where the van der Waals force can be obtained by differentiating (2) with respect to  $Z$ .

The potential energy of a many-body system comprising pairs of molecules, which is called the pair potential approximation,<sup>20</sup> is given as:

$$U = \frac{1}{2} \sum_{i,j=1, i \neq j}^N E(\rho_{ij}) \quad (3)$$

where  $\rho_{ij}$  denotes the distance between a surface element  $i$  and a surface element  $j$ . Therefore, the interaction energy between two TiO<sub>2</sub> molecules and a carbon nanotube can be obtained by:

$$U = \sum_{i=1}^2 E_{\text{tube-ball}}(\rho_i) + E_{\text{ball-ball}}(\rho) \quad (4)$$

where  $E_{\text{tube-ball}}$  is given as (2) with  $\rho_1^2 = b^2 + (z - Z)^2$  and  $\rho_2^2 = b^2 + (z - Z + Z_0)^2$  where  $Z_0$  is the equilibrium distance between two TiO<sub>2</sub> molecules. The term  $E_{\text{ball-ball}}$  is given as  $E_{\text{ball-ball}}(\rho) = -AP_6(\rho) + BP_{12}(\rho)$  where

$$\begin{aligned} P_n(\rho) &= \frac{4\pi^2 a^2 \eta_f^2}{\rho(2-n)(3-n)} \left( \frac{1}{(2a+\rho)^{n-3}} + \frac{1}{(-\rho)^{n-3}} \right. \\ &\quad \left. - \frac{1}{(2a-\rho)^{n-3}} - \frac{1}{\rho^{n-3}} \right) \end{aligned}$$

and, in this case,  $\rho = Z$ . Note that the analytical determinations can be found in Cox et al.<sup>21,22</sup> and Baowan et al.<sup>23</sup>

If we are to consider the configuration energetically favorable for TiO<sub>2</sub> nanoparticles to be encapsulated into one end of the carbon nanotube note that the interaction energy between two TiO<sub>2</sub> molecules and a carbon nanotube is lower than that between one TiO<sub>2</sub> molecule and a carbon nanotube; therefore the particles are likely to form a cluster or a chain before entering into the tube. Also note that in our experiments the radius of the carbon nanotube, 135 Å,<sup>18</sup> is smaller than that of the TiO<sub>2</sub>, 150 Å, as shown in Figure 1. This result is supported by our theoretical finding of encapsulation of TiO<sub>2</sub> nanoparticles into single-walled carbon nanotubes as shown in Figure 3(a).

Once the radius of the TiO<sub>2</sub> is assumed to be fixed, the relation between the suction energy, which is the driving energy from the van der Waals alone and the nanotube radii is determined. The authors found that, theoretically, TiO<sub>2</sub> nanoparticle starts to be encapsulated into the tube if its radius is around 2.8 Å smaller than that of the tube;

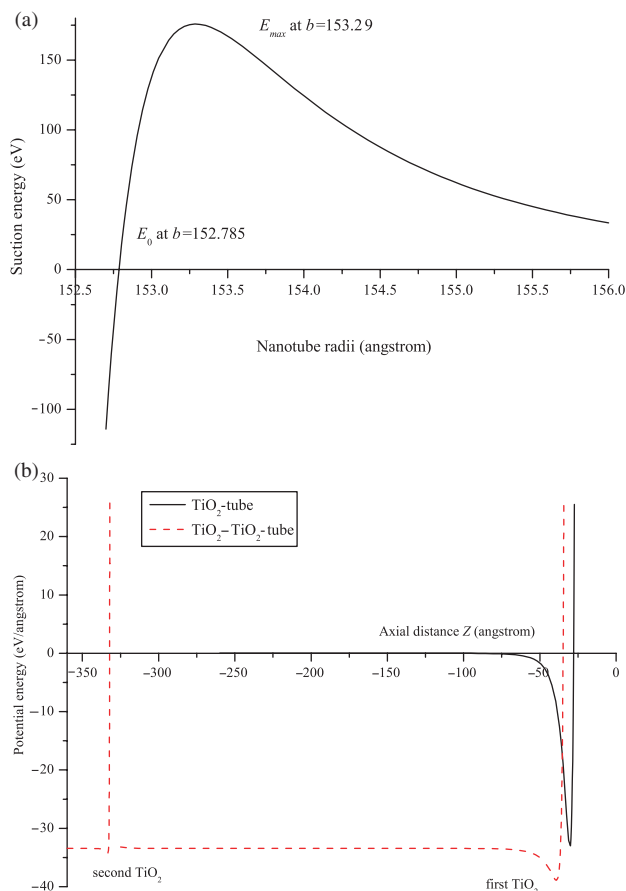


**Fig. 3.** Suction energy (a) and potential energy (b) for the TiO<sub>2</sub>-tube and for the TiO<sub>2</sub>-TiO<sub>2</sub>-tube.

the maximum suction energy occurs when the difference of their radii is around 3.3 Å. These two behaviors are unvarying by changing the radii. Hence this seems to suggest that the best case scenario for the experiment is when the radius of the particle and the radius of the tube are equal; therefore, for calculation purposes the two radii are assumed to be equal and are taken to be 150 Å. The parameters used in this model are given in Table I. Specifically, there are two different interactions for the interaction energy between TiO<sub>2</sub> and a carbon nanotube, which are C-Ti and C-O, so that the total energy can be obtained by:

$$U^{\text{tot}} = \frac{\eta_1}{3} \eta_2 U^*(A_{\text{C-Ti}}, B_{\text{C-Ti}}) + \frac{2\eta_1}{3} \eta_2 U^*(A_{\text{C-O}}, B_{\text{C-O}})$$

where  $U^*(A, B)$  is defined by  $U/AB$  and  $U$  is given as (2) and (4) for the interaction energy between a TiO<sub>2</sub> and a carbon nanotube, and for two TiO<sub>2</sub> molecules and a carbon nanotube, respectively. The constants for C, Ti, and O are taken from the work of Mayo et al.,<sup>24</sup> and the constants for the carbon nanotube are taken from the work of Girifalco et al.<sup>25</sup> The mixing rule<sup>26</sup> is undertaken to determine the constants for the coupling of the two atom species.

**Table I.** Lennard-Jones constants for C-TiO<sub>2</sub> system.

Interaction	$\epsilon$ (meV)	$\sigma$ (Å)	$A$ (eV $\times$ Å <sup>6</sup> )	$B$ (eV $\times$ Å <sup>12</sup> )
C-Ti	3.14	3.7588	35.38	99795.40
C-O	4.14	3.2531	19.61	23241.81
Graphene-graphene	3.83	2.39	15.2	24100

The potential energy (or the van der Waals force) is a short range energy (force), therefore the tube is assumed to be semi-finite in length and we can consider each side of the tube separately. Firstly, we calculate the interaction energy between TiO<sub>2</sub> and the tube. The numerical calculation is presented by the solid line in Figure 3(b). The minimum energy occurs at  $Z = Z_0 = -30.328$  Å, where the negative sign indicates the left hand side of the tube. Subsequently, in order to investigate the case of TiO<sub>2</sub>-TiO<sub>2</sub>-tube interaction, we fix the distance between the first TiO<sub>2</sub> molecule and the tube to be  $Z_0$ . The model is detailed in Figure 2(b) and the energy calculation is depicted by the dashed line in Figure 3(b). It is clearly seen from the comparison graphs that the energy level of TiO<sub>2</sub>-TiO<sub>2</sub>-tube interaction is lower than that of TiO<sub>2</sub>-tube interaction. As a result, the TiO<sub>2</sub> nanoparticles are likely to be together rather than alone when entering into the carbon nanotube. It should be noted that this continuum approach takes into account both armchair and zigzag carbon nanotubes because the discrete carbon atoms are assumed to be replaced by an average atomic distribution over each surface. In the experiments, multi-walled carbon nanotubes were used, and in the calculations we considered only the single-walled carbon nanotubes. This will not change the behavior of the system since the total potential energy can be obtained linearly by summing each pair of interaction as given in (3); consequently, only the magnitude of the energy will be changed.

### 3. CONCLUDING REMARKS

In this work, we have presented an explanation of our experimental results aimed at understanding why TiO<sub>2</sub> molecules aggregate at only one side of a carbon nanotube in order to be encapsulated into the tube, which is part of the main problem surrounding the encapsulation of TiO<sub>2</sub> nanoparticles into SWNT when using mainly applied mathematical modeling tools. We employed the Lennard-Jones potential to calculate the interaction energy, and we made the usual continuum approximation, in which the discrete carbon atoms are assumed to be replaced by an average distribution over each surface. The interaction energy between two TiO<sub>2</sub> molecules and the SWNT is theoretically found to be lower than that between one TiO<sub>2</sub> molecule and the SWCN. Therefore the particles are likely to form a cluster or a chain before entering into the tube. This result is supported by the experimental data. Hence our approach could be used to predict whether or not

TiO<sub>2</sub> particles might be sucked into a SWNT, which could become an important issue for applications involving drug delivery research.

Because some microscopic details and stochastic interactions, as well as fluctuations, are ignored, our method allows for calculations to be analytically performed and some theoretical predictions to be made. Although it is relatively less time consuming than other methods; it does require a geometrical and physical background of the nanoparticles studied. In comparison to other methods used for nanoscience studies (such as first principle calculations, molecular dynamics or Monte Carlo simulations), our applied mathematical modeling approach has not been widely used in this field. To the authors' knowledge, no work has been undertaken on mathematical modeling to describe the encapsulation behavior of TiO<sub>2</sub> nanoparticles into CNT. More work, such as the establishment of optimal conditions and more precise evaluations of encapsulation, is now progressing. Our current results, however, could give confidence to the high feasibility of developing new nano-scale materials.

**Acknowledgments:** The authors thank David Blyler for editing the manuscript and our biophysics group members for reading the manuscript and providing helpful comments. The authors gratefully thank the Nanomechanics Group at the University of Wollongong, Australia. This work is partially supported by The Center of Excellent in Mathematics, The Center of Excellence for Innovation in Chemistry (PERCH-CIC), The Thailand Center of Excellence in Physics (ThEP), The Thailand Research Fund (TRF), The Mahidol University Research Grant, The Commission on Higher Education (CHE), and The Ministry of Education.

## References

1. S. Iijima and T. Ichihashi, *Nature* 363, 603 (1993).
2. D. S. Bethune, C. H. Klang, M. S. de Vries, G. Gorman, R. Savoy, J. Vazquez, and R. Beyers, *Nature* 336, 605 (1993).
3. M. M. Calbi, M. W. Cole, S. M. Gatica, M. J. Bojan, and G. Stan, *Rev. Mod. Phys.* 73, 857 (2001).
4. Y. Maniwa, H. Kataura, M. Abe, A. Udaka, S. Suzuki, Y. Achiba, H. Kira, K. Matsuda, H. Kadowaki, and Y. Okabe, *Chem. Phys. Lett.* 401, 534 (2005).
5. A. N. Khlobystov, D. A. Britz, A. Ardavan, G. Andrew, and D. Briggs, *Phys. Rev. Lett.* 92, 245507 (2004).
6. A. L. Linsebigler, G. Lu, and J. T. Yates, *Chem. Rev.* 95, 735 (1995).
7. D. Chatterjee and S. Dasgupta, *J. Photochem. Photobiol. C* 6, 186 (2005).
8. C. Wei, W. Y. Lin, Z. Zainal, N. E. Williams, R. L. Smith, K. Rajeshwar, K. Zhu, and A. P. Kruzic, *Environ. Sci. Technol.* 28, 934 (1994).
9. R. J. Watts, S. H. Kong, M. P. Orr, G. C. Miller, and B. E. Henry, *Water Res.* 29, 95 (1995).
10. S. Lee, M. Nakamura, and S. Ohgaki, *J. Environ. Sci. Health A* 33, 1643 (1998).
11. H. Sakaia, E. Itob, R. X. Caia, T. Yoshiokab, Y. Kubotac, K. Hashimotoa, and A. Fujishima, *BBA-Gen. Subj.* 1201, 259 (1994).
12. D. M. Blake, P. C. Maness, Z. Huang, E. J. Wolfrum, J. Huang, and W. A. Jacoby, *Sep. Purif. Meth.* 28, 1 (1999).
13. A. V. Emeline, A. V. Frolov, V. K. Ryabchuk, and N. Serpone, *J. Phys. Chem. B* 107, 7109 (2003).
14. N. Serpone, *The Kirk-Othmer Encyclopedia of Chemical Technology*, Wiley, New York (1996).
15. C. Srinivasan and N. Somasundaram, *Current Sci.* 85, 1431 (2003).
16. J. C. Ireland, P. Klostermann, E. W. Rice, and R. Clark, *Appl. Environ. Microbiol.* 59, 1668 (1993).
17. M. Cho, H. Chung, W. Choi, and J. Yoon, *Appl. Environ. Microbiol.* 71, 270 (2005).
18. P. Singjai, S. Changsarn, and S. Thongtem, *Mater. Sci. Eng. A* 443, 42 (2007).
19. J. E. Lennard-Jones, *Proc. Phys. Soc.* 43, 461 (1931).
20. M. Rieth, *Nano-Engineering in Science and Technology: An Introduction to the World of Nano-Design*, World Scientific Publishing, Singapore (2003).
21. B. J. Cox, N. Thamwattana, and J. M. Hill, *Proc. R. Soc. A* 463, 461 (2007).
22. B. J. Cox, N. Thamwattana, and J. M. Hill, *Proc. R. Soc. A* 463, 477 (2007).
23. D. Baowan, N. Thamwattana, and J. M. Hill, *J. Phys. A: Math. Theor.* 4, 7543 (2007).
24. S. L. Mayo, B. D. Olafson, and W. A. Goddard, III, *J. Phys. Chem.* 94, 8897 (1999).
25. L. A. Girifalco, M. Hodak, and R. S. Lee, *Phys. Rev. B* 62, 13104 (2000).
26. J. O. Hirschfelder, C. F. Curtiss, and R. B. Bird, *Molecular Theory of Gases and Liquids*, John Wiley & Sons, Inc. (1954).

Received: 29 October 2009. Accepted: 16 December 2009.